Formation Control of Four-Legged Robots Using Discrete-Valued Inputs

Shinsaku Izumi, *Member, IEEE*, Kiko Shinagawa, Xin Xin, *Senior Member, IEEE*, and Taiga Yamasaki

***Abstract*—This letter addresses a formation control problem of four-legged robots with discrete-valued inputs. Four-legged robots have the potential for completing tasks on non-flat terrains, while their position control is achieved by switching between specific movements, i.e., discrete-valued signals. This implies that existing results assuming the use of continuous-valued inputs are not available. We present a solution to this control problem by combining conventional formation controllers with dynamic quantization. The resulting feedback system is then analyzed based on a performance index describing the difference between the systems with and without quantization. As a result, we can estimate the effects of the quantization on the behavior of the system and guarantee its stability.**

***Index Terms*—Distributed control, quantized systems, robotics.**

I. Introduction

FORMATION control of multi-robot systems—steering robots to form a desired configuration—has become a major topic in the field of control systems. The research has been motivated by various engineering applications, e.g., risky area surveillance and cooperative transportation using vehicles.

Although existing works on formation control have focused on omnidirectional [1], [2] and two-wheeled [3], [4] robots, and linear dynamical agents [5], we consider here *four-legged* robots. An example is shown in Fig. 1. This robot can perform forward, backward, and lateral movements and rotations using its four legs. The reason for considering four-legged robots is twofold. First, four-legged robots can easily travel on non-flat terrains compared to wheeled robots because they can adjust the height of the tip of each leg according to the terrains. This is especially advantageous in outdoor applications. Second, using four legs is reasonable with respect to stability and cost. In fact, it is difficult for two-legged robots to maintain stability while moving one leg, but using too many legs increases the cost of hardware and energy supply.

Manuscript received March 4, 2021; revised May 10, 2021; accepted May 26, 2021. Date of publication June 11, 2021; date of current version July 1, 2021. This work was supported in part by JSPS KAKENHI under Grant 19K15016. Recommended by Senior Editor L. Menini. *(Corresponding author: Shinsaku Izumi.)*

The authors are with the Faculty of Computer Science and Systems Engineering, Okayama Prefectural University, Okayama 719-1197, Japan (e-mail: izumi@cse.oka-pu.ac.jp; xxin@cse.oka-pu.ac.jp; taiga@cse.oka-pu.ac.jp).

Digital Object Identifier 10.1109/LCSYS.2021.3088683

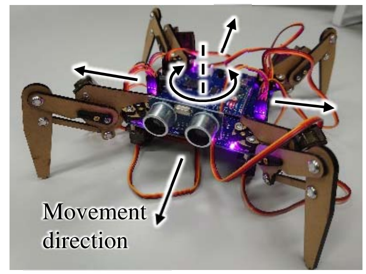

Fig. 1. Four-legged robot [6].

Meanwhile, controlling these robots through continuous-valued inputs is difficult. Using continuous-valued inputs requires four-legged robots to change their positions smoothly. However, this requirement is not satisfied because the robots are driven by the commands of specific movements [6], [7] and move by switching between these movements. This means that existing results assuming the use of continuous-valued inputs are not directly applicable to four-legged robots.

Thus, we aim to develop a framework for the formation control of four-legged robots through *discrete-valued* inputs corresponding to the aforementioned movement commands. The contributions of this letter are summarized as follows.

1) We present formation controllers using discrete-valued inputs for four-legged robots. Our controllers transform the control signals for omnidirectional robots into those for four-legged robots and quantize the transformed signals to satisfy the constraint of discrete values. In addition, the effects of the quantization on the resulting formation are mitigated through the feedback of the quantization error, i.e., the error between the quantized signal and the original signal. The performance of our controllers is demonstrated through a simulation.
2) We analyze the resulting feedback system based on a performance index to quantify the difference between systems with and without quantization. We reveal that an upper bound of the quantization error is given as a nonlinear function of the maximum magnitude of the signal to be quantized, and evaluate the performance index using this property. As a result, we can estimate the effects of the quantization on the resulting formation and ensure the stability of the feedback system.

At the end of this section, we comment on related works. The control of multi-robot (agent) systems with quantization was studied in, e.g., [8], [9]. Moreover, the performance analysis problem addressed in this letter is formulated based on [10]. However, four-legged robots were not handled in these works. In addition, from a technical point of view, the property of the quantization error in our feedback system is not trivial, unlike [10] where the property is directly given as that of uniform quantizers, making the performance analysis difficult. We reveal this property and obtain the main results from it, as mentioned above. Hence, our results are not straightforward consequences of those in [10].

Notation: Let $\mathbb{R}$ and $\mathbb{R}_+$ denote the real number field and the set of positive real numbers, respectively. The zero scalar and vector are both denoted by 0. The $n\times m$ zero matrix and the $n\times n$ identity matrix are represented by $0_{n\times m}$ and I_n, respectively. Let $\|\cdot\|$ denote the ∞-norms of vectors and matrices and let $\|\cdot\|_2$ denote the Euclidean norms of vectors. For the vectors u and v and the matrices U and V, $u\cdot v$ and $U\otimes V$ represent the inner product and the Kronecker product, respectively. For the vectors $x_1, x_2, \ldots, x_n \in \mathbb{R}^2$ and the set $\mathbb{I} := \{i_1, i_2, \ldots, i_m\} \subseteq \{1, 2, \ldots, n\}$, we define $[x_i]_{i\in\mathbb{I}} := [x_{i_1}^\top \; x_{i_2}^\top \; \cdots \; x_{i_m}^\top]^\top \in \mathbb{R}^{2m}$. We use $|\mathbb{S}|$ to represent the cardinality of the set $\mathbb{S}$. Finally, for the positive number c and the vector v, $\mathrm{sat}_c(v)$ denotes the saturation function ensuring that $|v_i| \le c$ for each element v_i of v.

II. Problem Formulation

Consider a multi-robot system Σ in a two-dimensional space. This consists of n four-legged robots modeled as

$$\begin{bmatrix} x_{i1}(t+1) \\ x_{i2}(t+1) \\ \theta_i(t+1) \end{bmatrix} = \begin{bmatrix} x_{i1}(t) \\ x_{i2}(t) \\ \theta_i(t) \end{bmatrix} + \begin{bmatrix} (\cos(\theta_i(t)+u_{i2}(t))(1-u_{i3}(t)) \\ (\sin(\theta_i(t)+u_{i2}(t))(1-u_{i3}(t)) \\ u_{i2}(t) \end{bmatrix.$$
$$\left.\begin{matrix} +\sin(\theta_i(t)+u_{i2}(t))u_{i3}(t))u_{i1}(t) \\ -\cos(\theta_i(t)+u_{i2}(t))u_{i3}(t))u_{i1}(t) \\ \end{matrix}\right], x_i(0) = x_i^0, \theta_i(0) = \theta_i^0, \quad (1)$$

where $i \in \{1, 2, \ldots, n\}$ is the robot index, $t \in \{0, 1, \ldots\}$ is discrete time, $[x_{i1}(t) \; x_{i2}(t)]^\top \in \mathbb{R}^2$ (denoted by $x_i(t)$) is the position, $\theta_i(t) \in (-\pi, \pi]$ is the orientation, $u_{i1}(t), u_{i2}(t) \in \mathbb{R}$ and $u_{i3}(t) \in \{0, 1\}$ are the control inputs, and x_i^0 and θ_i^0 are the initial values of $x_i(t)$ and $\theta_i(t)$, respectively. The inputs $u_{i1}(t)$ and $u_{i2}(t)$ determine the translational and rotational velocities, respectively, and $u_{i3}(t)$ determines the movement type. More precisely, $u_{i3}(t) = 0$ denotes a combination of rotation and forward (or backward) movement, and $u_{i3}(t) = 1$ denotes that of rotation and lateral movement, as shown in Fig. 2. Equation (1) is obtained by introducing $u_{i3}(t)$ to a continuous-time model of a two-wheeled robot to allow lateral movements and discretizing the resulting model.

We suppose that each robot i has the controller

$$K_i : \begin{cases} \xi_i(t+1) = f_{i1}(\xi_i(t), [x_j(t)-x_i(t)]_{j\in\mathbb{N}_i}, \theta_i(t)), \\ u_i(t) = f_{i2}(\xi_i(t), [x_j(t)-x_i(t)]_{j\in\mathbb{N}_i}, \theta_i(t)), \end{cases} \quad (2)$$

where $\xi_i(t) \in \mathbb{R}^m$ is the state, $[x_j(t)-x_i(t)]_{j\in\mathbb{N}_i} \in \mathbb{R}^{2|\mathbb{N}_i|}$ and $\theta_i(t)$ are the inputs, $u_i(t) \in \mathbb{R}^3$ is the output (i.e., $u_i(t) := [u_{i1}(t) \; u_{i2}(t) \; u_{i3}(t)]^\top$), and $f_{i1} : \mathbb{R}^m \times \mathbb{R}^{2|\mathbb{N}_i|} \times (-\pi, \pi] \to \mathbb{R}^m$ and $f_{i2} : \mathbb{R}^m \times \mathbb{R}^{2|\mathbb{N}_i|} \times (-\pi, \pi] \to \mathbb{R}^3$ are functions specifying the behavior of the controller. The set $\mathbb{N}_i \subset \{1, 2, \ldots, n\}$ is the index set of the neighboring robots, i.e., the robots whose *relative* positions can be observed by robot i. For simplicity, we assume that $\xi_i(0) = 0$. In addition, the elements $u_{i1}(t)$ and $u_{i2}(t)$ of the output $u_i(t)$ are restricted to discrete values, i.e., $u_{i1}(t) \in \{0, \pm s, \pm 2s, \ldots\}$ and $u_{i2}(t) \in \{0, \pm\pi/4, \pm\pi/2, \pm(3\pi)/4, \pi\}$ for the step size $s \in \mathbb{R}_+$. This implies that at each time step, the movement distance and direction of each robot are restricted to integer multiples of s and $\pi/4$, respectively.

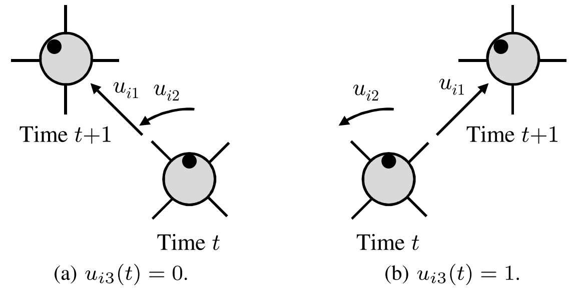

Fig. 2. Two examples of movements by robot i.

We describe the network topology of the system Σ using the time-invariant directed graph $G = (\mathbb{V}, \mathbb{E})$, where $\mathbb{V} := \{1, 2, \ldots, n\}$ and $\mathbb{E} \subset \mathbb{V}\times\mathbb{V}$ are the vertex and edge sets representing the robot indices and the information flow between the robots, respectively. Based on this notation, $\mathbb{N}_i$ is defined as $\mathbb{N}_i := \{j \in \mathbb{V} | (j, i) \in \mathbb{E}\}$.

Let $r_{ij} \in \mathbb{R}^2$ be the desired relative position of robot i in terms of robot j. Our problem is then formulated as follows.

Problem 1: For the multi-robot system Σ, suppose that the step size s and the desired relative positions r_{ij} $(i, j = 1, 2, \ldots, n)$ are given. Find controllers $K_1, K_2, \ldots, K_n$ (i.e., functions $f_{11}, f_{12}, f_{21}, \ldots, f_{n2}$) such that

$$\lim_{t\to\infty} (x_i(t) - x_j(t)) = r_{ij} \quad \forall (i, j) \in \mathbb{V}\times\mathbb{V} \quad (3)$$

for every initial state $(x_i^0, \theta_i^0) \in \mathbb{R}^2\times(-\pi, \pi]$ $(i = 1, 2, \ldots, n)$.

Three remarks on Problem 1 are given. First, it is impossible to achieve (3) exactly because $u_{i1}(t)$ and $u_{i2}(t)$ for each robot i are restricted to discrete values. Hence, we aim to achieve (3) approximately. Second, to develop a framework for adjusting the relative positions of the robots as the first step of research, we do not assume the existence of a leader to allow moving formations. Third, each robot can move in lateral directions using its four legs unlike two-wheeled robots, and thus this property should be used effectively. This and the discrete-valued input constraint are the main features of Problem 1.

III. Formation Control Using Discrete-Valued Inputs

This section presents our solution to Problem 1.

A. Proposed Controllers

A typical formation controller for each robot i is given by

$$K_{i0} : \tilde{u}_i(t) = -k \sum_{j\in\mathbb{N}_i} (x_i(t) - x_j(t) - r_{ij}), \quad (4)$$

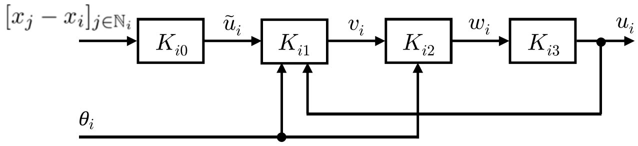

Fig. 3. Structure of the proposed controller K_i.

where $\tilde{u}_i(t) \in \mathbb{R}^2$ is the output (vector) whose elements represent the velocities in the x_{i1} and x_{i2} directions, and $k \in \mathbb{R}_+$ is the gain. However, the controller K_{i0} cannot be directly applied to Problem 1 because K_{i0} assumes that each robot is omnidirectional and that the control input can take continuous values. Therefore, we modify K_{i0} to a controller for the system (1) with the discrete-valued $u_{i1}(t)$ and $u_{i2}(t)$.

Based on this idea, we propose the controller K_i shown in Fig. 3 as a solution to Problem 1. This consists of K_{i0} and three blocks. The block K_{i1} is given by

$$K_{i1} : \begin{cases} \xi_i(t+1) = g(\theta_i(t), u_i(t)) - v_i(t), \\ v_i(t) = \mathrm{sat}_{\bar{v}}(-\xi_i(t) + \tilde{u}_i(t)), \end{cases} \tag{5}$$

where $\xi_i(t)$ is a two-dimensional vector (i.e., $m := 2$), $\theta_i(t)$, $u_i(t)$, and $\tilde{u}_i(t)$ are the inputs, $v_i(t) \in \mathbb{R}^2$ is the output, and $\mathrm{sat}_{\bar{v}}$ is the saturation function, as explained in Section I. The function $g : (-\pi, \pi] \times \mathbb{R}^3 \to \mathbb{R}^2$ returns the velocities in the x_{i1} and x_{i2} directions when applying $u_i(t)$ to robot i, i.e., $x_i(t+1) - x_i(t)$. The block K_{i2} is described by

$$K_{i2} : w_i(t) = \begin{bmatrix} \|v_i(t)\|_2 \\ \mathrm{arctan2}(v_{i2}(t), v_{i1}(t)) - \theta_i(t) \end{bmatrix}, \tag{6}$$

where $v_i(t) = [v_{i1}(t)\ \ v_{i2}(t)]^\top$ and $\theta_i(t)$ are the inputs, $w_i(t) \in \mathbb{R}^2$ is the output, and arctan2 represents the four-quadrant inverse tangent. Finally, K_{i3} is of the form

$$K_{i3} : u_i(t) = \begin{cases} [q(w_{i1}(t))\ \ 0\ \ 0]^\top, & \text{if } -\pi/8 \le w_{i2}(t) < \pi/8, \\ [q(w_{i1}(t))\ \ 0\ \ 0]^\top, & \text{if } -(5\pi)/8 \le w_{i2}(t) < -(3\pi)/8, \\ [q(w_{i1}(t))\ \ \pi/4\ \ 0]^\top, & \text{if } \pi/8 \le w_{i2}(t) < (3\pi)/8, \\ [q(w_{i1}(t))\ \ \pi/4\ \ 1]^\top, & \text{if } -(3\pi)/8 \le w_{i2}(t) < -\pi/8, \\ [q(-w_{i1}(t))\ \ 0\ \ 1]^\top, & \text{if } (3\pi)/8 \le w_{i2}(t) < (5\pi)/8, \\ [q(-w_{i1}(t))\ \ \pi/4\ \ 0]^\top, & \text{if } -(7\pi)/8 \le w_{i2}(t) < -(5\pi)/8, \\ [q(-w_{i1}(t))\ \ \pi/4\ \ 1]^\top, & \text{if } (5\pi)/8 \le w_{i2}(t) < (7\pi)/8, \\ [q(-w_{i1}(t))\ \ 0\ \ 0]^\top, & \text{otherwise}, \end{cases} \tag{7}$$

where $w_i(t) = [w_{i1}(t)\ w_{i2}(t)]^\top$ is the input, $u_i(t)$ is the output, and $q : \mathbb{R} \to \{0, \pm s, \pm 2s, \ldots,\}$ is the mid-tread uniform quantizer with the quantization interval s. In (7), we suppose that $w_{i2}(t) \in (-\pi, \pi]$.

The proposed controller K_i operates as follows. Since $\xi_i(t) = g(\theta_i(t-1), u_i(t-1)) - v_i(t-1)$ from (5), the state $\xi_i(t)$ stores the value of $g(\theta_i(t-1), u_i(t-1)) - v_i(t-1)$. Based on this value, K_{i1} modifies the signal $\tilde{u}_i(t)$ generated by K_{i0} and outputs it as $v_i(t)$. This is for mitigating the degradation of the control performance owing to the discrete-valued input constraint, and is inspired by the $\Delta\Sigma$ modulator [11], where $g(\theta_i(t), u_i(t)) - v_i(t)$ corresponds to the *quantization error*, i.e., the error between the resulting discrete-valued velocities of robot i and the original continuous-valued $v_i(t)$. The saturation function $\mathrm{sat}_{\bar{v}}$ in (5) is introduced to specify the maximum magnitude of the signal $v_i(t)$; the reason for this will be detailed in Section IV-B. The block K_{i2} calculates the desired translational and rotational velocities from $v_i(t)$ representing the desired velocities in the x_{i1} and x_{i2} directions. The block K_{i3} generates a control input $u_i(t)$ that satisfies the constraint of discrete values based on $w_i(t)$ from K_{i2}. The element $u_{i1}(t)$ is determined using the simple static quantizer q, and $u_{i2}(t)$ and $u_{i3}(t)$ are determined so that the resulting movement direction of robot i is closest to the desired one. Note that $u_{i2}(t)$ only has to take the values 0 and $\pi/4$ by switching between forward (or backward) and lateral movements, as shown in (7).

B. Illustrative Example

Consider the case of $n := 6$ and $s := 0.05$. The network topology G will be shown later. The desired formation is illustrated in Fig. 4(a), where the circles and the numbers $1, 2, \ldots, 6$ denote the robots and their indices, respectively. We use the controllers K_i $(i = 1, 2, \ldots, 6)$ described by (4)–(7) with $k := 0.05$ and $\bar{v} := 0.15$.

Fig. 4(b) and (c) show the initial and resulting formations, respectively, where the dots in the circles represent the orientations θ_i $(i = 1, 2, \ldots, 6)$, and the arrows represent the edges of the graph G. Fig. 5 shows the time evolution of the control input $u_1(t)$ for agent 1 as an example. These results indicate that the proposed controllers achieve a formation similar to the desired one even under the discrete-valued input constraint. Moreover, from Fig. 5(b) and (c), we can confirm that $u_{12}(t)$ only takes the values 0 and $\pi/4$, and that $u_{13}(t) = 1$, i.e., the lateral movement, is often chosen.

Remark 1: The proposed controllers are designed without the knowledge of the physical parameters of the robots, such as the length of their legs; thus, they are robust against the uncertainties in the parameters.

IV. Theoretical Analysis

In this section, we analyze the feedback system with the proposed controllers. Although the control objective (3) and the proposed controllers are described by using the relative positions of the robots, we perform the analysis focusing on the absolute positions to use existing results on multi-agent control. In addition, to focus on the relation between the quantization of the control inputs and the system behavior, we do not consider the effects of the error between the input and output of $\mathrm{sat}_{\bar{v}}$ in (5). In this case, $\mathrm{sat}_{\bar{v}}$ simply provides the maximum magnitude of $v_i(t)$ as a function of $\bar{v}$. The effects of the error can be avoided by choosing a smaller k in (4) so that the input of $\mathrm{sat}_{\bar{v}}$ does not exceed $\bar{v}$.

A. Convergence of Feedback System Without Quantization

We first consider the case where $u_{i1}(t)$ and $u_{i2}(t)$ are not quantized in (7). More precisely, we suppose that $u_i(t)$ can be chosen to achieve the desired velocities specified by $w_i(t)$. In this case, the following result is obtained.

Lemma 1: For the feedback system given by (1) and (4)–(7), suppose that r_{ij} $(i, j = 1, 2, \ldots, n)$ are given and that

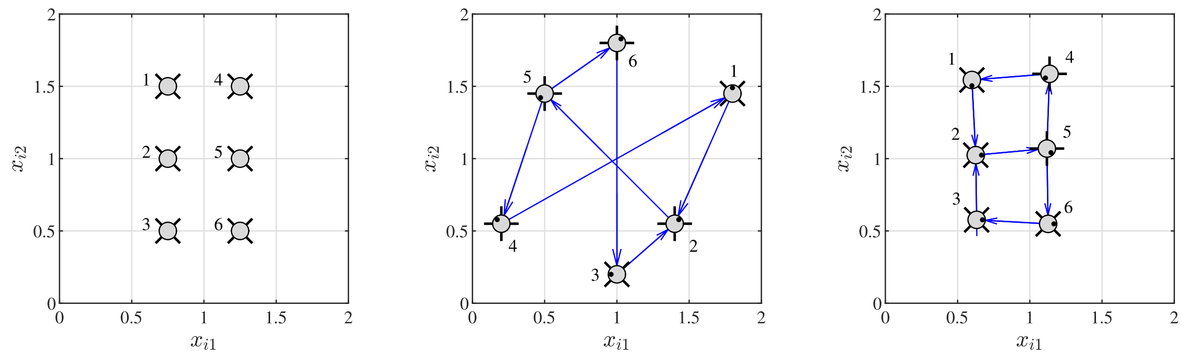

(a) Desired formation. (b) Initial formation. (c) Resulting formation (at $t = 120$).

Fig. 4. Desired, initial, and resulting formations.

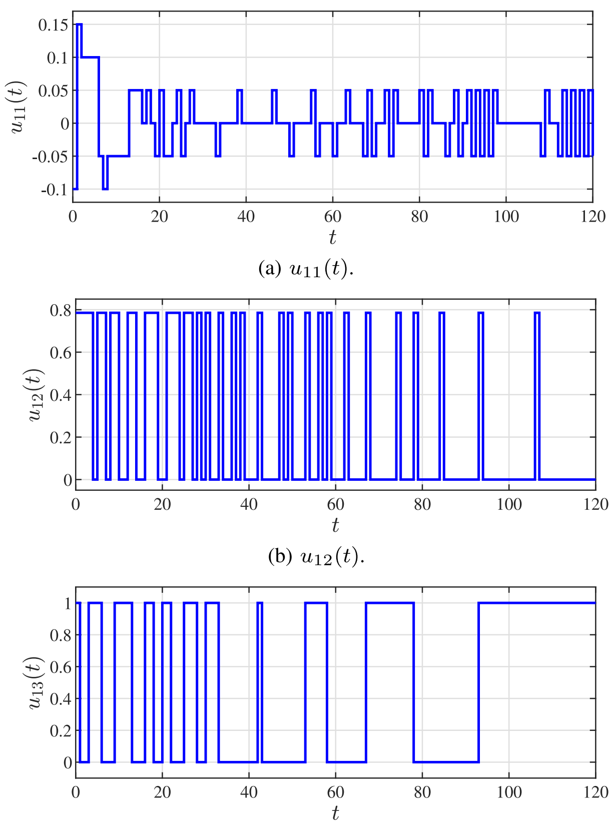

(a) $u_{11}(t)$. (b) $u_{12}(t)$. (c) $u_{13}(t)$.

Fig. 5. Time evolution of $u_1(t)$.

$u_{i1}(t)$ and $u_{i2}(t)$ are not quantized in (7). If the following two conditions hold, (3) holds for every $(x_i^0, \theta_i^0) \in \mathbb{R}^2 \times (-\pi, \pi]$ $(i = 1, 2, \ldots, n)$.

(C1) The graph G has a directed spanning tree.

(C2) The gain k satisfies $k < 1/d_{\max}$, where $d_{\max} \in \mathbb{R}_+$ is the maximum degree of G.

Proof: Under the assumption that $u_{i1}(t)$ and $u_{i2}(t)$ are not quantized in (7), $\xi_i(t) \equiv 0$ holds for every $i \in \mathbb{V}$ because $\xi_i(0) = 0$ for every $i \in \mathbb{V}$ and there is no quantization error. This, together with (4)–(7) and the assumption, implies that the controller K_i steers robot i according to (4). Thus, from (1) and (4), the position $x_i(t)$ of each robot i is updated as

$$x_i(t+1) = x_i(t) - k \sum_{j \in \mathbb{N}_i} (x_i(t) - x_j(t) - r_{ij}). \tag{8}$$

By letting $r_i \in \mathbb{R}^2$ be the desired absolute position of robot i and applying $\Delta x_i(t) := x_i(t) - r_i$ to (8), we obtain

$$\Delta x_i(t+1) = \Delta x_i(t) - k \sum_{j \in \mathbb{N}_i} (\Delta x_i(t) - \Delta x_j(t)), \tag{9}$$

where $r_{ij} = r_i - r_j$ is used. For (9) with $i = 1, 2, \ldots, n$,

$$\lim_{t \to \infty} (\Delta x_i(t) - \Delta x_j(t)) = 0 \quad \forall (i, j) \in \mathbb{V} \times \mathbb{V} \tag{10}$$

implies (3). Noting that (9) is a typical consensus algorithm, we can show that (10) holds for every $\Delta x_i(0) \in \mathbb{R}^2$ $(i = 1, 2, \ldots, n)$ subject to conditions (C1) and (C2) [12]. This and the fact that (8) does not depend on θ_i^0 $(i = 1, 2, \ldots, n)$ prove the lemma. ∎

Lemma 1 indicates that the proposed controllers achieve the desired formation if the control inputs are not quantized. Hence, we only need to consider the effects of quantization on the behavior of the feedback system.

B. Effects of Quantization

1) Analysis Problem: Let $x(t) \in \mathbb{R}^{2n}$ denote the positions of n robots, i.e., $x(t) := [x_1^\top(t)\ x_2^\top(t)\ \cdots\ x_n^\top(t)]^\top$, and let $x^*(t) \in \mathbb{R}^{2n}$ denote $x(t)$ for the proposed controllers without the quantization of $u_{i1}(t)$ and $u_{i2}(t)$ in (7). We then address the following problem formulated based on [10].

Problem 2: For the feedback system given by (1) and (4)–(7), suppose that the step size s, the desired relative positions r_{ij} $(i, j = 1, 2, \ldots, n)$, and the parameter $\bar{v}$ of $\mathrm{sat}_{\bar{v}}$ in (5) are given. Evaluate the performance index

$$E := \sup_{x(0) \in \mathbb{R}^{2n}} \sup_{\tau \in \{0,1,\ldots\}} \|x(\tau) - x^*(\tau)\|. \tag{11}$$

In this problem, E quantifies the difference between the feedback systems with and without the quantization of the control inputs. A smaller value of E means that the effects of the quantization on the system behavior are smaller.

2) Characterization of Quantization Error: To solve Problem 2, for the feedback system with the proposed controllers, we characterize the quantization error $e_i(t) := g(\theta_i(t), u_i(t)) - v_i(t)$ $(i \in \mathbb{V})$ by the following lemma.

Lemma 2: For the feedback system given by (1) and (4)–(7), suppose that s and $\bar{v}$ are given. Then,

$$\|e_i(t)\| \leq \sqrt{\left(\frac{s}{2}\right)^2 + \left(1 - \cos\left(\frac{\pi}{8}\right)\right)\left(4\bar{v}^2 + \sqrt{2}s\bar{v}\right)} \quad (12)$$

holds for every $i \in \mathbb{V}$ and $t \in \{0, 1, \ldots\}$.

Proof: By the definition of $e_i(t)$, we obtain

$$\begin{aligned}\|e_i(t)\|_2^2 &= \|g(\theta_i(t), u_i(t)) - v_i(t)\|_2^2 \\ &= (g(\theta_i(t), u_i(t)) - v_i(t)) \cdot (g(\theta_i(t), u_i(t)) - v_i(t)) \\ &= g(\theta_i(t), u_i(t)) \cdot g(\theta_i(t), u_i(t)) \\ &\quad - 2g(\theta_i(t), u_i(t)) \cdot v_i(t) + v_i(t) \cdot v_i(t) \\ &= \|g(\theta_i(t), u_i(t))\|_2^2 - 2\|g(\theta_i(t), u_i(t))\|_2 \\ &\quad \times \|v_i(t)\|_2 \cos\phi_i(t) + \|v_i(t)\|_2^2 \end{aligned} \quad (13)$$

for each $i \in \mathbb{V}$, where $\phi_i(t) \in \mathbb{R}$ is the angle between the vectors $g(\theta_i(t), u_i(t))$ and $v_i(t)$. It follows from (1), (6), and (7) that $|\|g(\theta_i(t), u_i(t))\|_2 - \|v_i(t)\|_2| \leq s/2$ and $|\phi_i(t)| \leq \pi/8$ for every $i \in \mathbb{V}$ and $t \in \{0, 1, \ldots\}$. Applying these to (13) yields

$$\begin{aligned}\|e_i(t)\|_2^2 &\leq \|g(\theta_i(t), u_i(t))\|_2^2 - 2\|g(\theta_i(t), u_i(t))\|_2 \\ &\quad \times \|v_i(t)\|_2 \cos\left(\frac{\pi}{8}\right) + \|v_i(t)\|_2^2 \\ &= (\|g(\theta_i(t), u_i(t))\|_2 - \|v_i(t)\|_2)^2 + 2\|g(\theta_i(t), u_i(t))\|_2 \\ &\quad \times \|v_i(t)\|_2 - 2\|g(\theta_i(t), u_i(t))\|_2\|v_i(t)\|_2 \cos\left(\frac{\pi}{8}\right) \\ &\leq \left(\frac{s}{2}\right)^2 + 2\left(1 - \cos\left(\frac{\pi}{8}\right)\right)\|g(\theta_i(t), u_i(t))\|_2\|v_i(t)\|_2 \\ &\leq \left(\frac{s}{2}\right)^2 + 2\left(1 - \cos\left(\frac{\pi}{8}\right)\right)\left(\|v_i(t)\|_2 + \frac{s}{2}\right)\|v_i(t)\|_2. \end{aligned} \quad (14)$$

Therefore, it follows from $\mathrm{sat}_{\bar{v}}$ in (5) that

$$\begin{aligned}\|e_i(t)\|_2^2 &\leq \left(\frac{s}{2}\right)^2 + 2\left(1 - \cos\left(\frac{\pi}{8}\right)\right)\left(\sqrt{2}\bar{v} + \frac{s}{2}\right)\sqrt{2}\bar{v} \\ &= \left(\frac{s}{2}\right)^2 + \left(1 - \cos\left(\frac{\pi}{8}\right)\right)\left(4\bar{v}^2 + \sqrt{2}s\bar{v}\right) \end{aligned} \quad (15)$$

for each $i \in \mathbb{V}$. This proves the lemma because $\|\cdot\| \leq \|\cdot\|_2$ by the definition of the norms. ■

Noting that $\bar{v}$ corresponds to the magnitude of the signal $v_i(t)$, we see from Lemma 2 that $\|e_i(t)\|$ would increase with an increase in the magnitude of $v_i(t)$. This means that $e_i(t)$ is not guaranteed to be bounded if $\mathrm{sat}_{\bar{v}}$ is not contained in (5). This is because the locations that robot i can reach in one time step are not given as a uniform lattice in the (x_{i1}, x_{i2}) plane under the constraint on $u_{i1}(t)$ and $u_{i2}(t)$ considered here. However, by setting the maximum magnitude of $v_i(t)$ using $\mathrm{sat}_{\bar{v}}$, we can derive an upper bound of $\|e_i(t)\|$ as (12). This property of $e_i(t)$ is different from that in [10].

3) Main Results: Now, we present a solution to Problem 2. By a discussion similar to that presented in the proof of Lemma 1, $x^*(t+1)$ is obtained by vectorizing (8), i.e.,

$$x^*(t+1) = x^*(t) - k(L \otimes I_2)x^*(t) + kb, \quad (16)$$

where $L \in \mathbb{R}^{n\times n}$ is the graph Laplacian of the graph G and $b := [\sum_{j\in\mathbb{N}_1} r_{1j}^\top \ \sum_{j\in\mathbb{N}_2} r_{2j}^\top \ \cdots \ \sum_{j\in\mathbb{N}_n} r_{nj}^\top]^\top$. We can rewrite (16) as

$$x^*(t+1) = \tilde{P}x^*(t) + kb, \quad (17)$$

where $\tilde{P} := P \otimes I_2$ for the Perron matrix $P := I_n - kL$. Similarly, from (1) and (4)–(7), $x(t+1)$ is derived as

$$\begin{bmatrix} x(t+1) \\ \xi(t+1) \end{bmatrix} = \begin{bmatrix} \tilde{P} & -I_{2n} \\ 0_{2n\times 2n} & 0_{2n\times 2n} \end{bmatrix}\begin{bmatrix} x(t) \\ \xi(t) \end{bmatrix} + \begin{bmatrix} e(t) + kb \\ e(t) \end{bmatrix} \quad (18)$$

for $\xi(t) := [\xi_1^\top(t) \ \xi_2^\top(t) \ \cdots \ \xi_n^\top(t)]^\top$ and $e(t) := [e_1^\top(t) \ e_2^\top(t) \ \cdots \ e_n^\top(t)]^\top$.

From (16) and (18), the following theorem is obtained.

Theorem 1: For the feedback system given by (1) and (4)–(7), suppose that s, r_{ij} $(i, j = 1, 2, \ldots, n)$, and $\bar{v}$ are given. Then, the following inequality holds:

$$E \leq \left(1 + \sum_{\ell=0}^{\infty}\left\|\tilde{P}^{\ell+1} - \tilde{P}^{\ell}\right\|\right) \times \sqrt{\left(\frac{s}{2}\right)^2 + \left(1 - \cos\left(\frac{\pi}{8}\right)\right)\left(4\bar{v}^2 + \sqrt{2}s\bar{v}\right)}. \quad (19)$$

Proof: From (17), $x^*(\tau)$ can be calculated as

$$x^*(\tau) = \tilde{P}^\tau x(0) + \sum_{\ell=0}^{\tau-1}\tilde{P}^{\tau-\ell-1}kb, \quad (20)$$

where $x^*(0) = x(0)$ is used. In addition, (18) yields

$$x(\tau) = \tilde{P}^\tau x(0) + \sum_{\ell=0}^{\tau-1}\tilde{P}^{\tau-\ell-1}(-\xi(\ell) + e(\ell) + kb), \quad (21)$$

$$\xi(\tau) = e(\tau - 1) \quad \forall\tau \in \{1, 2, \ldots\}. \quad (22)$$

Substituting $\xi(0) = 0$ and (22) into (21) provides

$$x(\tau) = \tilde{P}^\tau x(0) + \sum_{\ell=0}^{\tau-1}\tilde{P}^{\tau-\ell-1}kb + \sum_{\ell=0}^{\tau-2}\left(\left(\tilde{P}^{\tau-\ell-1} - \tilde{P}^{\tau-\ell-2}\right)e(\ell)\right) + e(\tau - 1). \quad (23)$$

From (20) and (23), $\|x(\tau) - x^*(\tau)\|$ is evaluated as

$$\begin{aligned}&\|x(\tau) - x^*(\tau)\| \\ &= \left\|\sum_{\ell=0}^{\tau-2}\left(\left(\tilde{P}^{\tau-\ell-1} - \tilde{P}^{\tau-\ell-2}\right)e(\ell)\right) + e(\tau - 1)\right\| \\ &\leq \sum_{\ell=0}^{\tau-2}\left\|\left(\tilde{P}^{\tau-\ell-1} - \tilde{P}^{\tau-\ell-2}\right)e(\ell)\right\| + \|e(\tau - 1)\| \\ &\leq \sum_{\ell=0}^{\tau-2}\left\|\tilde{P}^{\tau-\ell-1} - \tilde{P}^{\tau-\ell-2}\right\|\|e(\ell)\| + \|e(\tau - 1)\| \\ &\leq \left(1 + \sum_{\ell=0}^{\tau-2}\left\|\tilde{P}^{\tau-\ell-1} - \tilde{P}^{\tau-\ell-2}\right\|\right) \\ &\quad \times \sqrt{\left(\frac{s}{2}\right)^2 + \left(1 - \cos\left(\frac{\pi}{8}\right)\right)\left(4\bar{v}^2 + \sqrt{2}s\bar{v}\right)}, \end{aligned} \quad (24)$$

where the last inequality follows from Lemma 2. The right-hand side of (24) is a monotonically non-decreasing function with respect to $\tau \in \{0, 1, \ldots\}$, and does not depend on $x(0)$. This fact and (11) prove the theorem. ■

Theorem 1 provides an upper bound of the performance index E. Because P^ℓ converges as $\ell \to \infty$ under (C1) and

(C2) [12], $\tilde{P}^\ell$ converges as $\ell \to \infty$ due to $\tilde{P}^\ell = P^\ell \otimes I_2$. This implies that $\|\tilde{P}^{\ell+1} - \tilde{P}^\ell\|$ in (19) approaches zero as $\ell \to \infty$, which means that the upper bound in (19) is finite. From this and Lemma 1, under (C1) and (C2), the feedback system is stable in the sense that $x(t)$ is bounded for $\xi(0) = 0$ and every $(x_i^0, \theta_i^0) \in \mathbb{R}^2 \times (-\pi, \pi]$ $(i = 1, 2, \ldots, n)$.

For comparison, we consider the case where the quantization error $e_i(t)$ is not fed back in the proposed controller K_i. This can be treated as $\xi_i(t) \equiv 0$ in (5). In this case, the following theorem is obtained.

Theorem 2: In the same situation as that of Theorem 1, assume that $\xi_i(t) \equiv 0$ for every $i \in \mathbb{V}$. Then, the following inequality holds:

$$E \leq \left(\sum_{\ell=0}^{\infty}\left\|\tilde{P}^\ell\right\|\right)\sqrt{\left(\frac{s}{2}\right)^2 + \left(1 - \cos\left(\frac{\pi}{8}\right)\right)\left(4\bar{v}^2 + \sqrt{2}s\bar{v}\right)}. \tag{25}$$

Proof: The assumption and (18) yield

$$x(t+1) = \tilde{P}x(t) + e(t) + kb. \tag{26}$$

Hence, $x(\tau)$ is derived as

$$x(\tau) = \tilde{P}^\tau x(0) + \sum_{\ell=0}^{\tau-1}\tilde{P}^{\tau-\ell-1}(e(\ell) + kb). \tag{27}$$

By using (27) instead of (23) in the proof of Theorem 1, we can prove the theorem. ∎

Theorem 2 gives an upper bound of E when the quantization error is not fed back. By a discussion similar to the above, we see that the upper bound in (25) is infinite. Thus, the aforementioned stability of the feedback system is not guaranteed, unlike in the original case. From this result, we conclude that the feedback of the quantization error leads to an improvement in the performance in the sense of an upper bound of E and the guarantee of the stability of the system.

4) Example: We reconsider the example in Section III-B. In this example, E is evaluated as $E \leq 0.3422$ from Theorem 1. Meanwhile, the simulation result shown in Fig. 4 yields $\sup_{\tau \in \{0,1,\ldots,120\}} \|x(\tau) - x^*(\tau)\| = 0.03429$. This validates Theorem 1. Moreover, for the corresponding result when the quantization error is not fed back, $\sup_{\tau \in \{0,1,\ldots,120\}} \|x(\tau) - x^*(\tau)\| = 2.221$ is obtained. Therefore, in this example, the proposed controllers improve the accuracy of the resulting formation by feeding back the quantization errors.

Remark 2: If $\xi(0) \neq 0$, a term depending on $\xi(0)$ is added to the right-hand side of (19). However, also in this case, we can show that $x(t)$ is bounded for every $(x_i^0, \theta_i^0) \in \mathbb{R}^2 \times (-\pi, \pi]$ $(i = 1, 2, \ldots, n)$ by a discussion similar to the above. In this sense, the proposed controllers are robust against the error on $\xi(0)$.

Remark 3: Our results will be extended to the case where the network topology G is time-varying in the following way. First, we can show the convergence of the feedback system without the quantization of the control inputs from results (see, e.g., [12]) on the consensus for the time-varying topologies. Then, by evaluating E for the feedback system with time-varying $\tilde{P}$ and b in a way similar to that given in this section, we will be able to obtain results similar to Theorems 1 and 2.

Remark 4: We restrict $u_{i2}(t)$ to integer multiples of $\pi/4$ by considering the tradeoff between utilizing the mobility of four-legged robots and reducing the implementation cost. However, we will be able to handle the more general quantization interval, i.e., $u_{i2}(t) \in \{0, \pm\pi/p, \pm(2\pi)/p, \ldots, \pm((p-1)\pi)/p, \pi\}$ for the positive integer p. This is performed by modifying (7) based on the value of p and characterizing $e_i(t)$ for the resulting feedback system similar to Lemma 2. In this case, the upper bound in (12) will decrease as p increases because the quantization interval becomes smaller.

V. Conclusion

In this letter, we addressed a formation control problem of four-legged robots under discrete-valued input constraints. For this problem, we presented distributed controllers based on dynamic quantization and analyzed the resulting feedback system. As a result, it was demonstrated that the feedback of the quantization errors helps to improve the performance of the system and guarantee its stability.

There are some directions for future research. One example is to analyze the performance on the relative positions and centroid of robots. Another example is to extend our framework to the case of leader-follower formations.

References

[1] G. Freudenthaler and T. Meurer, "PDE-based multi-agent formation control using flatness and backstepping: Analysis, design and robot experiments," *Automatica*, vol. 115, May 2020, Art. no. 108897.

[2] L. Wang, J. Xi, M. He, and G. Liu, "Robust time-varying formation design for multiagent systems with disturbances: Extended-state-observer method," *Int. J. Robust Nonlinear Control*, vol. 30, no. 7, pp. 2796–2808, 2020.

[3] N. Zoghlami, R. Mlayeh, L. Beji, and A. Abichou, "Finite-time consensus for controlled dynamical systems in network," *Int. J. Control*, vol. 91, no. 4, pp. 813–826, 2018.

[4] S. Izumi and S. Azuma, "Chemotaxis-inspired control for multi-agent coordination: Formation control by two types of chemotaxis controllers," *New Gener. Comput.*, vol. 38, no. 2, pp. 303–324, 2020.

[5] F. A. Yaghmaie, R. Su, F. L. Lewis, and L. Xie, "Multiparty consensus of linear heterogeneous multiagent systems," *IEEE Trans. Autom. Control*, vol. 62, no. 11, pp. 5578–5589, Nov. 2017.

[6] Bit Trade One. *Quad Crawler*, Accessed: Mar. 4, 2021. [Online]. Available: https://bit-trade-one.co.jp/adcrbt/ (in Japanese).

[7] M. M. U. Atique, M. R. I. Sarker, and M. A. R. Ahad, "Development of an 8DOF quadruped robot and implementation of inverse kinematics using Denavit-Hartenberg convention," *Heliyon*, vol. 4, no. 12, 2018, Art. no. e01053.

[8] D. V. Dimarogonas and K. H. Johansson, "Stability analysis for multi-agent systems using the incidence matrix: Quantized communication and formation control," *Automatica*, vol. 46, no. 4, pp. 695–700, 2010.

[9] Y. Wang, L. He, and C. Huang, "Adaptive time-varying formation tracking control of unmanned aerial vehicles with quantized input," *ISA Trans.*, vol. 85, pp. 76–83, Feb. 2019.

[10] Y. Minami, S. Azuma, and T. Sugie, "An optimal dynamic quantizer for feedback control with discrete-valued signal constraints," in *Proc. 46th IEEE Conf. Decis. Control*, 2007, pp. 2259–2264.

[11] A. V. Oppenheim, R. W. Schafer, and J. R. Buck, *Discrete-Time Signal Processing*, 2nd ed. Upper Saddle River, NJ, USA: Prentice Hall, 1998.

[12] W. Ren and R. W. Beard, *Distributed Consensus in Multivehicle Cooperative Control*. London, U.K.: Springer, 2008.